sciendo

Civil and Environmental Engineering
Vol. 20, Issue 1, 364-376, DOI: 10.2478/cee-2024-0028

BEHAVIOR OF FATIGUE DAMAGED REINFORCED CONCRETE ONE-WAY SLABS REPAIRED WITH CFRP SHEETS

Mohammed O. HAMEED[1,*], Raid A. DAUD[2]

[1] M.Sc. Student, Dept. of Civil Engineering, College of Engineering, Al-Nahrain University, Baghdad, Iraq.
[2] Assist. Prof., Ph.D., Dept. of Civil Engineering, College of Engineering, Al-Nahrain University, Baghdad Iraq.
[*] corresponding author: st.mohammed.a.h.f@nahrainuniv.edu.iq

Abstract

The results of experimental research involving nine one-way slabs are detailed in this report. The objective was to investigate the impact of different parameters on the structural performance of these slabs in their absence and with strengthening. Externally bonded CFRP sheets strengthened six of the nine slabs; the three remaining slabs served as control specimens. Before subjecting the specimens to monotonic loading, pre-fatigue damage of 50% and 70% repeated loading was induced. An exhaustive assessment was conducted on each slab, in which it was compared to its control slab. Several crucial elements were incorporated into the evaluation, including the ultimate load capacity, the reason for failure, crack patterns, and load-deflection curves. Examining these metrics was intended to provide insight into the efficacy and structural performance of the employed fortification technology. Compared to unenhanced reinforced concrete slabs (control slab), the highest stresses on slabs supported with bonded CFRP sheets are between 20 and 44% better. Compared to the control slab, an almost 70% reduction in deflection was observed. The flexural performance of compromised reinforced concrete slabs repaired with this technology can be brought up to date and enhanced.

Keywords:

One-way slabs;
CFRP sheet;
Monotonic loading;
Fatigue damage;
Repairing;

1 Introduction

The most advanced method of upgrading or rehabilitation available today is external strengthening using contemporary composite materials, most notably (CFRP) [1]. Because it is so simple to install, the Externally Bonded Reinforcement (EBR) approach is gaining popularity. For this system, design guidelines and standards have been established [2]. Masonry or concrete structures can be strengthened with fiber-reinforced polymer or FRP. R.C. members' flexural capability is enhanced by the efficacy of widening CFRP. Several studies have demonstrated the benefits of the EB-FRP strengthening technique in raising the flexural capacity of R.C. components. The research findings were influenced by fatigue-loading circumstances [3-6]. Because of its limited bearing capacity for deformation under tensile stress, concrete has a reputation for being a brittle material. Potential causes of the formation of these tensile stresses include mechanical loads, adverse responses, and environmental loading. Cracks that develop as a result of these forces frequently negatively affect the performance of concrete. Most reinforced concrete slabs and beams will have cracks at some point. Restoring the damaged parts' structural capability requires strengthening and retrofitting [7–12].

In addition to affecting the bonding agent and structural elements' performance, fatigue-loading stresses may cause cracks. The inevitable cracking of any structural part is a fact of life. Restoring their flexural capabilities requires strengthening or repairing the injured parts [13–18]. The slab worked wonderfully as a rigid diaphragm system because of its enormous size, thickness, and span, contributing to its outstanding stiffness. Strengthening the slab's ductility ratio allows it to endure more deflection before giving way [19–21]. Several processes are possible to reinforce and retrofit steel plates, cement grout, epoxy injection, fiber-reinforced polymers, Ferro-cement, and other reinforced concrete structural

© Author(s) 2024. This work is distributed under the Creative Commons BY 4.0 license (https://creativecommons.org/licenses/by/4.0/).

components. Before selecting an appropriate repair procedure, it is necessary to consider several factors [22–26], including the extent of the damage, the material required for restoration, the cost of construction, and the available time. The functionality of reinforced concrete (R.C.) specimens undergoing one-way CFRP repair was investigated. The three variables under investigation were the CFRP sheet's breadth, thickness, and magnitude of fatigue stress. Despite being preloaded with CFRP, the CFRP-fixed specimens exhibited fewer cracks than the preloaded specimens. Enhanced structural bonding, decreased maintenance expenses, a reduced requirement for installers, a straightforward installation process, and a high strength-to-weight ratio are just some of the advantages that FRP systems have demonstrated in comparison to more traditional strengthening techniques. Engineers and academics have conducted many studies to advance this technology as its capabilities have expanded [27]. FRP, or fiber-reinforced polymer, is an adaptable substance capable of reinforced concrete and masonry structures. A potential method for improving the flexural strength of reinforced concrete elements is to augment the girth of carbon fiber-reinforced polymer (CFRP) [28–30]. The CFRP-EB technique repaired cracked slabs. The principal aim of this study is to evaluate the influence of the fatigue damage ratio on three structural parameters: the failure mechanism, crack pattern, and deflection profile.

2 Experimentation plan

2.1 Material and Specimen Testing

Experiments were conducted on nine one-way reinforced concrete slabs with varying percent load conditions (ranging from 50% to 70% of the ultimate load). The slabs were subjected to repeated loads to induce fatigue damage before strengthening, and then monotonic loading was applied until failure. Three of the five one-way slabs did not have CFRP sheets strengthening them, and the others had. The test slab specimens are uniformly 150 mm deep, 600 mm wide, and 1300 mm long. Their blueprint followed the guidelines outlined in the ACI 318-19 standard [31]. Standard steel bars with a diameter of 4Ø10 mm running longitudinally and 6Ø10 mm running perpendicularly were used to reinforce each one-way slab. Every slab has a 25-mm transparent concrete cover for the flexural steel bars. Concerning the specimens fortified using externally bonded CFRP sheets, two of the six slabs were subjected to a 70% repeated load, while the others were subjected to a 50% repeated load. The nominal specimen attributes, including concrete strength, load arrangement, CFRP detail, and others, are summarized in Tab. 1. For the samples tested in a one-way slab, Fig. 1 shows the nominal cross-sections and bottom views, including details of CFRP sheets.

Table 1: Ratios used in the elements of the frame.

Specimen symbols	Strengthening description	Width of CFRP sheet [mm]	Thickness of CFRP sheet [mm]	Cross-Area of CFRP sheet [mm^2]	Length of CFRP sheet [mm]	Repeated loading [%]	Distribution strip	Compressive strength [MPa]
S1-C	Control	…	…		…	…	…	35.92
SW2-50R	Without	…	…		…	50%	…	35.92
SW3-70R	Without	…	…		…	70%	…	36.2
SS4-50R	strengthening	100	0.17	34	1000	50%	Two strips	36.2
SS5-50R	strengthening	150	0.17	51	1000	50%	Two strips	36.2
SS6-50R	strengthening	100	0.34	68	1000	50%	Two strips	36.5
SS7-50R	strengthening	100	0.51	102	1000	50%	Two strips	36.5
SS8-70R	strengthening	100	0.17	34	1000	70%	Two strips	36.7
SS9-70R	strengthening	150	0.17	51	1000	70%	Two strips	36.7

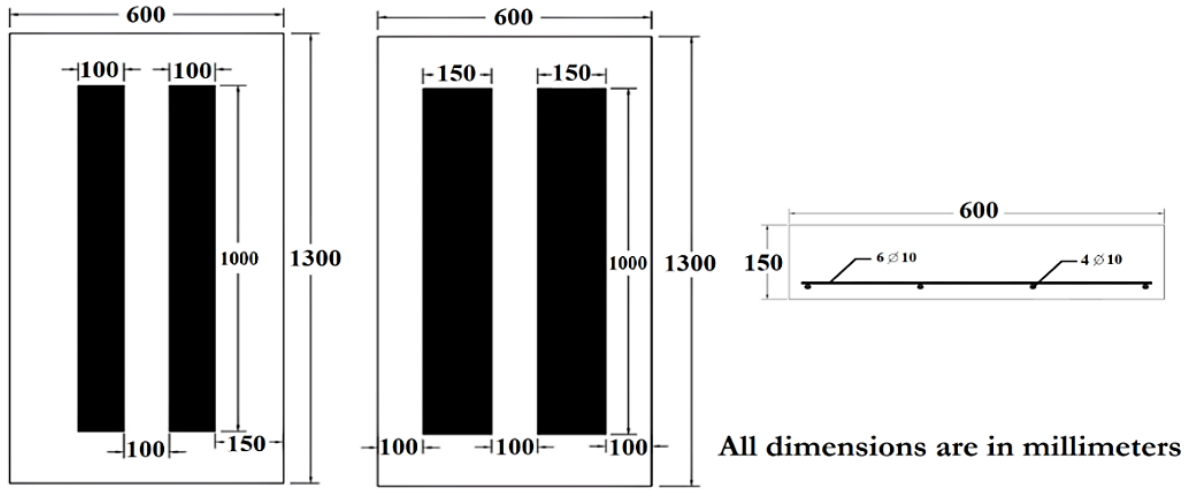


Fig. 1: Detailed bottom view with CFRP sheets and cross-sectional information.

Exhaustive details about the concrete material are provided in Table 2. Table 3 lists the proportions of the mixture necessary to generate one cubic meter of concrete. Even though 35 MPa was the intended compressive strength, the result was 35.08 MPa. The measured value of strength was lower than the objective value. Table 4 presents the tensile test results conducted on the steel bar. To attain the intended degree of compaction, specimens were organized into three strata through the utilization of a vibrator. After one day, the slabs were removed from their matrix and submerged in water for the next twenty-eight days. After that, the specimens were transferred to a facility with expertise in civil engineering for ten days before the testing commenced. The Teknowrap 300 polymer, reinforced with carbon fiber, possessed a tensile strength of 4900 MPa and an elastic modulus of 230 MPa. The nomenclature assigned to the structural adhesive substance utilized was Teknobond 300. Decomposing this adhesive substance into two discrete constituents, denoted as parts A and B, is possible. The ratio utilized to combine these two components was 3.34A to 1B, as shown in Table 5 and Table 6.

Table 2: Mix the amount of concrete.

Property	Experimentally	ACI 318 M (2019)
Strength in compression (*f*'c) [MPa]	35.08	-
Tensile splitting strength (*f 'ct*) [MPa]	3.36	3.09 ($0.5\sqrt{f'c}$)
Rupture modulus (*f r*) [MPa]	6.8	3.83 ($0.62\sqrt{f'c}$)
Elasticity modulus (Ec) [GPa]	28.135	($4700\sqrt{fc'}$)

Table 3: Characteristics of mix design.

Compressive strength target [MPa]	Compressive strength as measured [MPa]	The ratio of water to cement	Cement [kg/m^3]	Sand [kg/m^3]	Gravel [kg/m^3]	Super. percentage by water of cement	Water [kg or liters]
35	35.08	0.243	370	787	1150	3	90

Table 4: Results of steel bars' tensile tests.

Property	Test outcomes
Standard steel bar DIA. [mm]	10
Real steel bars DIA. [mm]	10.06
Yield strength [MPa]	619
Ultimate strength [MPa]	732
Elasticity modulus [GPa]	200

Table 5: Mechanical properties of CFRP sheet.

Properties	Teknowrap 300
Strength of tensile [MPa]	≥ 4900
Elasticity modulus [GPa]	230
Strain at break [min.] %	2.1
Thickness [mm]	0.17
Unit Weight [g/m^2]	300

Table 6: Epoxy resin's mechanical characteristics.

Properties at 7days and 25°C	Teknbond 300
Strength of tensile [MPa]	≥ 30
Elasticity modulus [MPa]	10000
Strength in compression [MPa]	≥ 80
Strength of bond [MPa]	≥ 4
Ratio of mixing	3.34A:1B

2.2 Experimental configuration

Before preparing for the testing process, the specimens were painted in white color to observe the first cracks during the application of loads on the samples shown in Fig. 3. Photographic and schematic depictions of the experimental test setup are displayed in Fig. 4. Four channel section columns make up the steel testing frame. The load was cantered all over the mid-span of each specimen, which was applied using cyclic hydraulic jacks with a 2000 kN capacity mounted on a steel universal H-section beam. The load transfer system was used to transfer the loads to the concrete specimens, which consist of a single longitudinal rigid steel spreader beam and a steel plate of 50 mm width, as in Fig. 5, as a line load, to disperse the actuator load. Steel rollers that should have allowed for a line support distance of 50 mm from the slab ends supported the concrete slabs measuring 1300 x 600 x 150 mm. The loading is monotonic and occurs at 12.1 kN/min, while the repeated loading is at a 1.9 kN/min rate. Before the test started, the applied loads were measured straight from the hydraulic jacks and calibrated using load cells. The machine creates an Excel sheet with the results (Displacement).



Fig. 3: Specimens paint process.

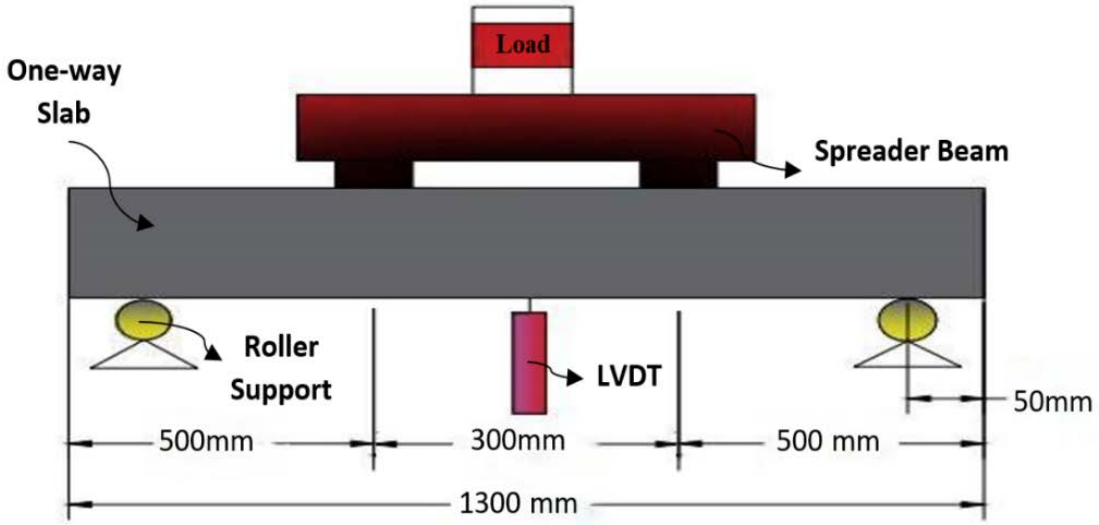


Fig. 4: Test Setup Schematic (front view).



Fig. 5: Hydraulic testing machine.

2.3 Experimental result

This section details the crack pattern, load capacity, and failure mode for all experimentally tested specimens. Experimental results about failure and crack stresses are presented in Table 7. The test results for group A indicated that the ultimate loads (Pu) of one-way slabs without strengthening (SW2-50R and SW3-70R) decreased by around 9.42% and 19.2%, respectively, when fatigue-damaged ratios reached 50% and 70%. In comparison, the ultimate load (Pu) of the control slab (S1-C) subjected to monotonic loads was unchanged. In the absence of strengthening techniques, this illustrates the detrimental effect fatigue damage has on the load-bearing capacity of the slabs. Group B's ultimate load (Pu) increased significantly due to the implementation of strengthening techniques for slabs subjected to a fatigue-compromised ratio of 50%. The transformation of the CFRP sheet configuration resulted in notable enhancements in the ultimate loads of SS4-50R, SS5-50R, SS6-50R, and SS7-50R concerning the ultimate load of S1-C, which was evaluated under monotonic loading conditions, of 22.44%, 33.19%, 35.89%, and 44.4%, respectively. This shows how well the CFRP sheet designs reduce the negative impacts of fatigue degradation and raise the slab's load-bearing capability. When strengthening procedures were applied to slabs that had sustained a 70% fatigue damage ratio, group C showed a significant improvement in ultimate loads (Pu). When SS8-70R and SS9-70R's final loads were compared to S1-C's, the CFRP sheet configurations for these two models produced increases of 20.49%

and 29.79%, respectively. These results show that CFRP sheet designs can help boost the load-bearing capability of the slab even in the presence of severe fatigue degradation.

The two specimens in Group A, SW2-50R and SW3-70R, have not undergone any strengthening processes. SW2-50R had a fatigue damage ratio of 50%, while SW3-70R had a fatigue damage ratio of 70%. The failure mechanism and crack pattern found at 50% and 70% fatigue damage ratios are shown in Fig. 6. SW3-70R had a significantly higher incidence of first cracks than SW2-50R and the control slab (S1-C). Compared to SW2-50R and the control slab, the first crack in SW3-70R occurred at an earlier stage, between 25% and 27% of the ultimate load—the majority of the cracks developed in the slabs' tensile area. Flexural failure was identified as the fault mechanism for both slabs.

Group B consists of four specimens: SS4-50R, SS5-50R, SS6-50R, and SS7-50R. CFRP sheets were used to strengthen each of these specimens. Fig. 7 graphically depicts the failure modes and crack pattern at a fatigue damage ratio of 50%. Debonding between the CFRP sheet and the concrete caused the failure of structures SS4-50R, SS6-50R, and SS7-50R. Simultaneously, minute cracks were discovered on the concrete substrate's bottom surface. SS5-50R, on the other hand, experienced shear failure. The first flexural crack in SS5-50R developed first at the zone of maximum moment, which is the middle third of the tension side of the slab. These cracks occurred when the tensile strains in the bottom fiber of the concrete surpassed the rupture modulus. Nonetheless, when the final degree of stress neared, cracks emerged quickly near the support, leading to the slab's collapse.

Group C includes specimens of SS8-70R and SS9-70R strengthened with CFRP sheets. Fig. 8 depicts the observed mechanism of failure and crack patterns, notably at a fatigue damage ratio of 70%. The failure of SS8-70R and SS9-70R may be traced to debonding between the CFRP sheet and the concrete surface. Minor cracks were also discovered on the concrete substrate's bottom surface. It is worth noting, however, that the cracks in SS8-70R were more widespread. This is due to the test extending beyond the point at which the CFRP sheets failed, causing flexural failure in the mid-span area of the slabs.

Table 7: The experimental results.

Group No.	Specimen symbols	Description	Width of CFRP sheet [mm]	Thick. of CFRP sheet [mm]	Cross-Area of CFRP strip [mm^{2}]	Ultimate Load (P u) [kN]	Cracking Load (Pcr) [kN]	Pcr / P u [%]	Percentage of the change in Ultimate Load compared with Ref.	Percentage of the change in Cracking Load compared with Ref.	Mode of failure
...	S1-C	Control slab Ref.	…	…	…	122	33	27	…	…	Flexural
Group A	SW2-50R	50% damage Without strengthening	…	…	…	110.5	29	26.2	-9.42	-12.12	Flexural
	SW3-70R	70% damage Without strengthening	…	…	…	98.5	25	23.3	-19.2	-24.24	Flexural
Group B	SS4-50R	50% damage, 2 strips of CFRP sheet strengthening	100	0.17	34	149.38	32	21.4	+22.44	-3.03	Debonding
	SS5-50R	50% damage, 2 strips of CFRP sheet strengthening	150	0.17	51	162.5	35	21.5	+33.19	+6.06	Flexural-shear
	SS6-50R	50% damage, 2 strips of CFRP sheet strengthening	100	0.34	68	165.79	36	21.7	+35.89	+9.09	Debonding
	SS7-50R	50% damage, 2 strips of CFRP sheet strengthening	100	0.51	102	176.17	37	21	+44.4	+12.12	Debonding
Group C	SS8-70R	70% damage, 2 strips of CFRP sheet strengthening	100	0.17	34	147	31	21.0	+20.49	-6.06	Debonding
	SS9-70R	70% damage, 2 strips of CFRP sheet strengthening	150	0.17	51	158.35	35	22.1	+29.79	+6.06	Debonding

S: slab, C: control, W: without strengthening, S: strengthening, (1-2-3…9): number of slabs, 50-70 R: (50-70) repeated loads.

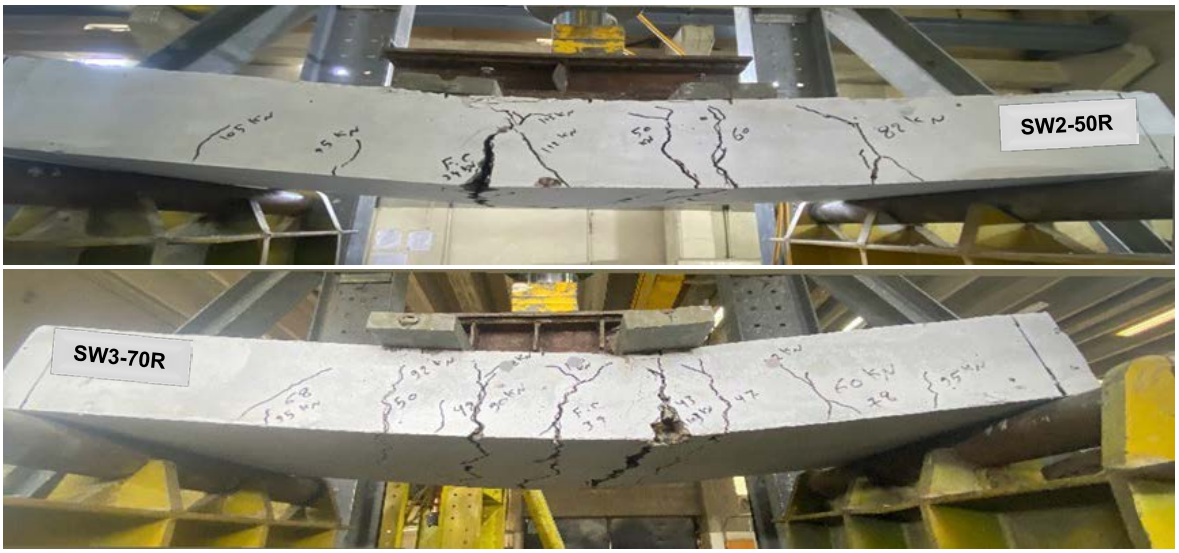


Fig. 6: Failure mode and Crack pattern (1) SW2-50R (2) SW3-70R.



Fig. 7: Failure mode and Crack pattern for SS4-50R, SS5-50R, SS6-50R, and SS7-50R.

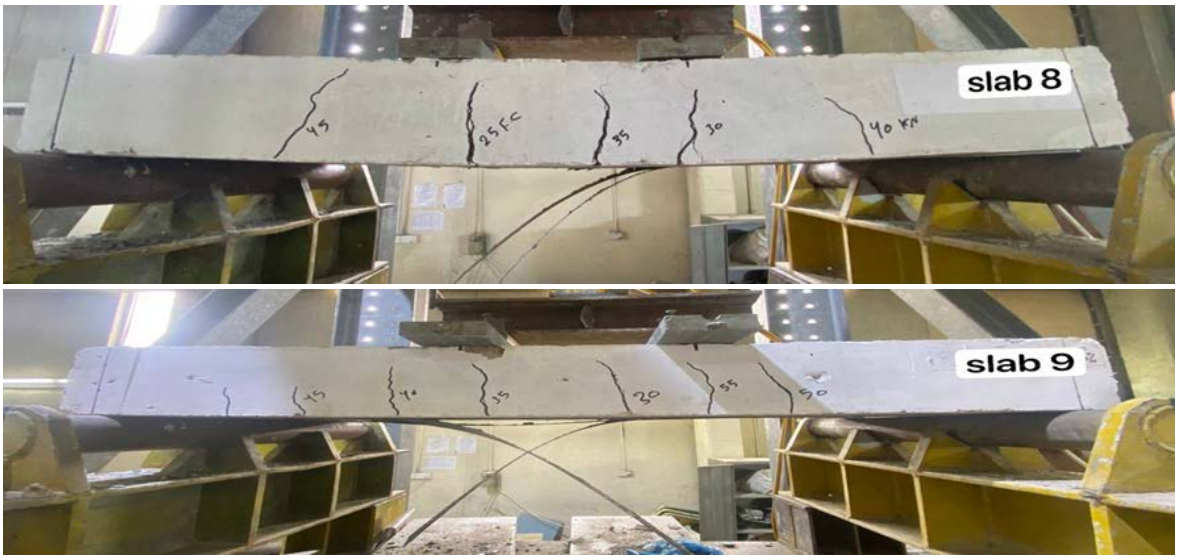


Fig. 8: Failure mode and Crack pattern for SS8-70R and SS9-70R.

2.4 Load-deflection behavior

The load-deflection curve is a significant statistic for explaining the overall behavior of structural components. When a specimen is progressively loaded, it will generally rise in the elastic region initially, then faster when cracks form, and continue to develop until the tension steel reinforcement yields. This is because cracks are an unavoidable by-product of the loading process. The slope of the curve will begin to decrease at that point, and the test will be declared complete when the deflection starts to climb without an accompanying increase in the load applied. Figs. 9–11 illustrate the load-deflection responses for all specimens (groups) studied. The load-deflection curve is a significant statistic for explaining the overall behavior of structural components. When a specimen is progressively loaded, it will generally rise in the elastic region initially, then faster when cracks form, and continue to develop until the tension steel reinforcement yields. This is because cracks are an unavoidable by-product of the loading process. The slope of the curve will begin to decrease at that point, and the test will be declared complete when the deflection starts to climb without an accompanying increase in the load applied. Figs. 9–11 illustrate the load-deflection responses for all specimens (groups) studied.

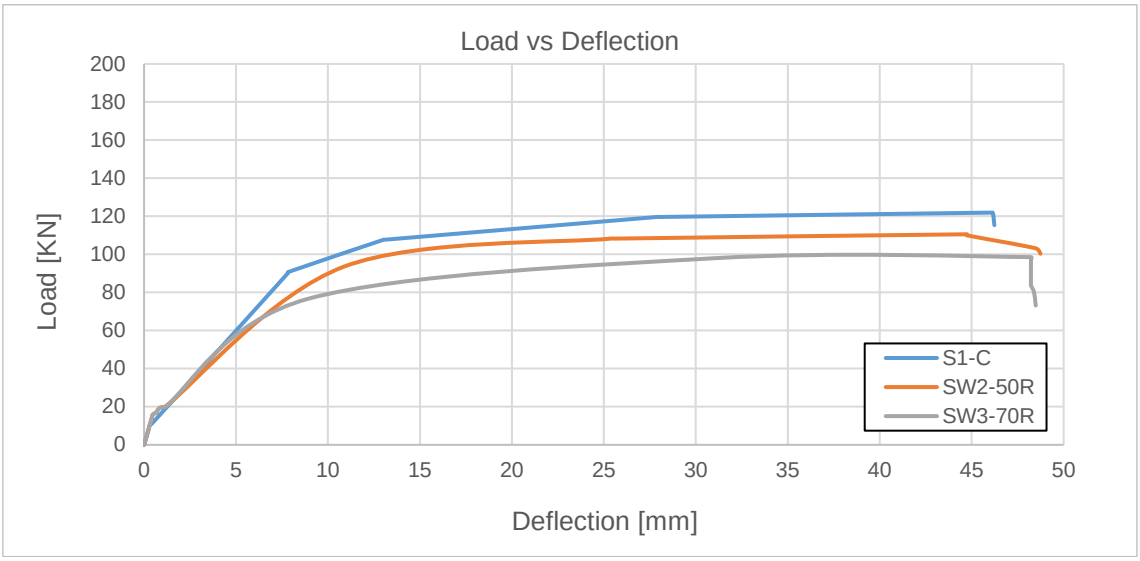


Fig. 9: The load-deflection curve for Group A compared with the control slab (S1-C).

The figure shows that all slabs have the same stiffness inside the elastic zone. When subjected to the same amount of stress, SW3-70R has lower stiffness than SW2-50R and the control slab. The stiffness difference may be attributable to the fact that SW3-70R has a fatigue damage ratio that is 70% greater than SW2-50R, which has a fatigue damage ratio of 50%. The fatigue damage affecting the slab

reduces its total stiffness and modulus of elasticity. Despite their variances, both slabs have comparable features and shapes. Implementing strengthening methods on slabs with a fatigue damage ratio of 50% significantly increased the ultimate load (Pu). It was evaluated under monotonic loading circumstances, and the ultimate loads for SS4-50R, SS5-50R, SS6-50R, and SS7-50R (Group B) were higher than those for S1-C (the control slab). The improvements were 22.44%, 33.19%, 35.89%, and 44.4%, respectively. Furthermore, there was a 72%, 75%, 74%, and 75% reduction in deflection, respectively. The enhancements were made feasible by changing the configuration of the CFRP sheets. This demonstrates that CFRP sheet designs may assist in achieving the aims of enhancing the load-bearing capacity of the slabs and reducing the negative impacts of fatigue degradation.

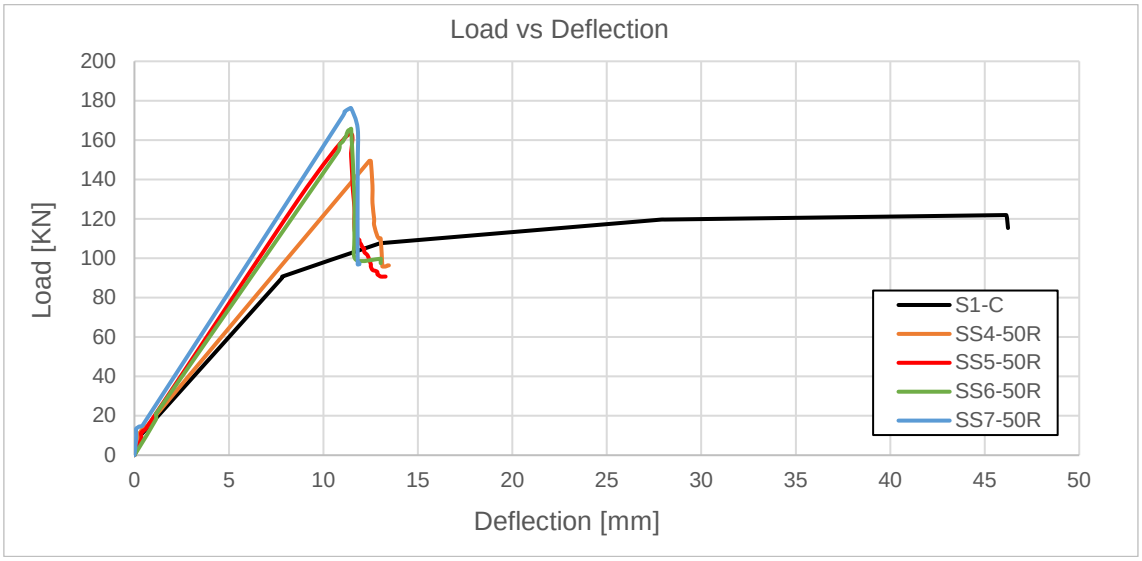


Fig. 10: The load-deflection curve for Group B compared with the control slab (S1-C).

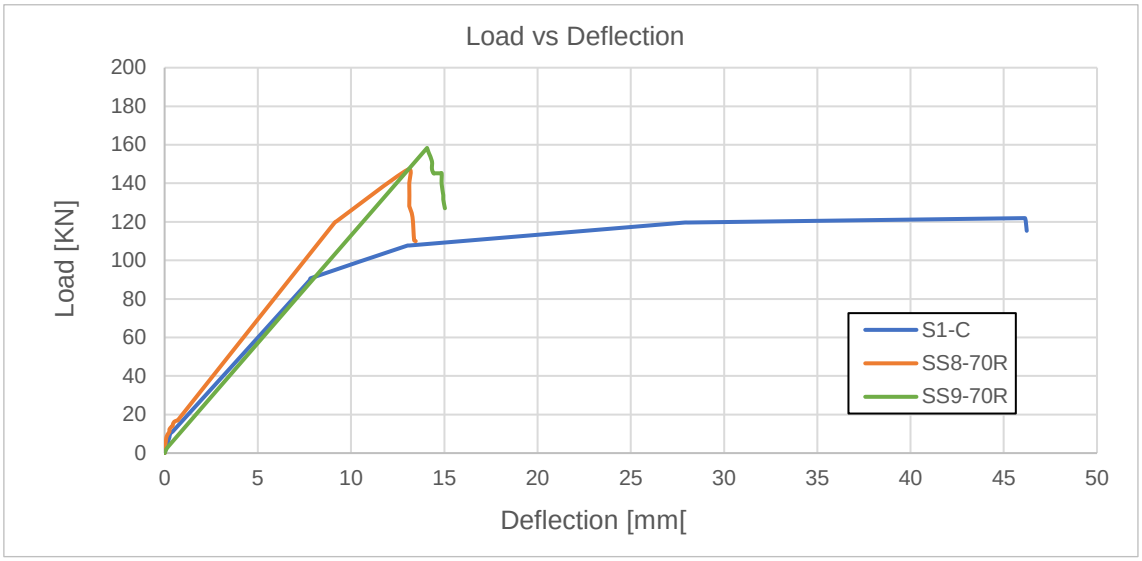


Fig. 11: The load-deflection curve for Group C compared with the control slab (S1-C).

When compared to the ultimate load and deflection at failure of S1-C (control slab), which was evaluated under monotonic loading circumstances, the ultimate loads for SS8-70R and SS9-70R (Group C) improved by 20.49% and 29.79%, respectively, and deflection lowered by 71% and 69%, respectively. On the other hand, the presence of CFRP sheets effectively resisted the applied flexural force, as shown by the persistence of the load-deflection curve with a constant slope. This behavior indicates the beneficial contribution of CFRP strengthening to structural integrity and slab load-carrying capacity. When a CFRP sheet increased stiffness and decreased deflection values, the influence of strengthening was apparent. Finally, the study shows that composite fiber sheets using the externally bonded (EB) technique might be a viable and practical alternative for strengthening damaged concrete

structures. Furthermore, the findings demonstrated that the CFRP region is essential in increasing the ultimate load, whether by increasing the width or thickness. Carbon fibers were consequently crucial in slab repairs. The load-deflection curve for all slab strengthening by different configurations of CFRP sheet (SS4-50R, SS5-50R, SS6-50R, SS7-50R, SS8-70R, and SS9-70R) was presented in Fig. 12.

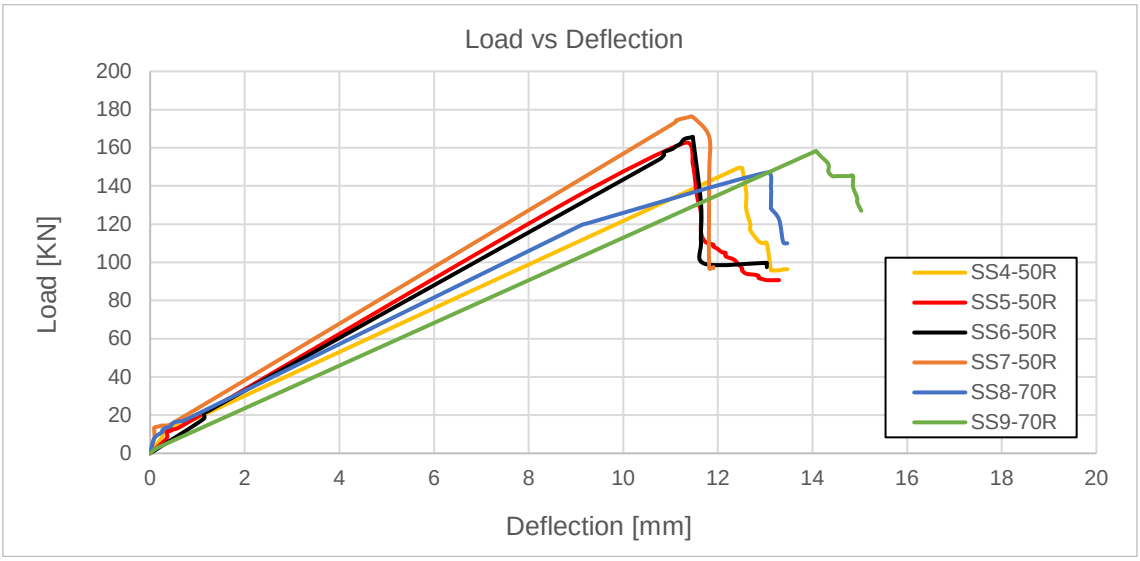


Fig. 12: The curve of load-deflection for all slabs strengthened by CFRP sheets.

Among the one-way slabs investigated in this research, SS7-50R provided the most favorable performance. The ultimate load capacity was 176.17 MPa, and the deflection was 11.46 mm. In contrast to the control surface, the ultimate load capacity improves by 44.4%. The exceptional performance of the SS7-50R is due to the exact arrangement of the used CFRP sheets. This monolith has a maximum area of 102 mm^2 of CFRP sheet. Three layers of CFRP sheet were used, with each layer being 1000 mm long, 100 mm wide, and 0.17 mm thick. The judicious arrangement and placement of these CFRP layers significantly increased load capacity in SS7-50R. Overall, our findings show that the chosen CFRP Repairing design enhances the fatigue-resistant structural performance of one-way slabs, notably slab (SS7-50R).

3 Energy absorption capacity

The system must have a significant amount of energy absorption capacity to be robust. This indicates that the system must be able to hold the initial kinetic energy provided by the impulse as potential energy without failing. This point should be limited below the deformation capacity since it is the site with the most significant displacement and the region with the maximum potential energy. The total area below the load-deflection curve at ultimate failure is computed to indicate energy absorption [32-34]. The deformability index DI [35] defines deformability as the ratio of the material's deflection to the final deflection at a fracture. This ratio is then subtracted from the final deflection. [36, 37] Equation 1 may be used to get the deformability index.

$$DI = \mathrm{r} = \frac{\Delta u - \Delta cr}{\Delta cr} \quad (1)$$

Tab. 8 presents the energy absorption and deformability index values for the slabs in this inquiry and all of the factors required to compute them.

Table 8: Efficiency of Slabs in Ductility and Energy Absorption.

Specimen symbols	Deflection at failure [mm]	Deflection at Crack [mm]	Energy absorption	Deformability index
S1-C	46	2.8	4797.8	15.42
SW2-50R	45	2.8	4575.9	15.07
SW3-70R	42	2.4	4033.3	16.5
SS4-50R	12.51	2.65	1089.6	3.72
SS5-50R	11.29	2.5	1180	3.51
SS6-50R	11.47	2.5	1129.8	3.59
SS7-50R	11.5	2.65	1142.8	3.34
SS8-70R	13.03	2	1159.1	5.51
SS9-70R	14.07	4.5	1262.2	2.13

4 Conclusions

The following conclusions may be drawn from the experimental data given in this work:

1) According to the test results, at fatigue damaged ratios of 50% and 70%, the ultimate loads (Pu) of one-way slabs without strengthening (SW2-50R and SW3-70R) decreased by approximately 9.42% and 19.2%, respectively, when compared to the ultimate load of the control slab (S1-C) tested under monotonic loads. This demonstrates the detrimental effect of fatigue degradation on the capacity of slabs to sustain loads without strengthening techniques.

2) Using strengthening procedures to slabs with a fatigue-damaged ratio of 50% significantly increases ultimate load (Pu). The ultimate loads for SS4-50R, SS5-50R, SS6-50R, and SS7-50R improved by 22.44%, 33.19%, 35.89%, and 44.4%, respectively, when the configuration of CFRP sheets was changed, compared to the ultimate load of S1-C, which was evaluated under monotonic loading circumstances. This demonstrates the effectiveness of CFRP sheet designs in increasing the load-carrying capacity of the slab and limiting the negative impacts of fatigue degradation.

3) Using strengthening procedures to slabs with a fatigue-damaged ratio of 70% resulted in significant increases in ultimate loads (Pu). The adjustments to the arrangement of CFRP sheets for SS8-70R and SS9-70R resulted in ultimate load increases of 20.49% and 29.79%, respectively, compared to the ultimate load of S1-C. These results emphasize the advantages of CFRP sheet designs in increasing the load-carrying capability of the slab, even in the presence of severe fatigue degradation.

4) The flexural failure crack pattern was consistent across all slab specimens strengthening with external CFRP sheets. Flexural cracks first occurred at the center-focused load's maximal moment zone. As the weight progressed through the slab, the fissures widened and ultimately reached the slab's upper face. The crack becomes more significant and broader until the CFRP collapses (debond from the CFRP).

5) The use of CFRP sheets as external strengthening in one-way slabs greatly influences the crack pattern of reinforced concrete one-way slabs by delaying the onset of the crack and limiting its width.

6) The effect of CFRP sheet width is greater that of CFRP sheet thickness because, in comparison to SS4-50R (which has a width of 100 mm), SS5-50R has a width of 150 mm (0.17 mm thick), increasing the ultimate load by 8.78%. Comparing SS6-50R (100mm width) to SS4-50R (100mm width), the thickness of the two layers is 0.34, increasing the ultimate load by 10.98% (twice the quantity).

Acknowledgment

My sincere appreciation goes out to Al-Nahrain University's technical personnel for their help with this experimental investigation.

References

[1] ABDULAH, M. D.: Behavior of Reinforced Height Strengthened Concrete One-Way Slabs Strengthened with CFRP Sheets. Engineering and Technology Journal 33.3 Part (A) Engineering (2015).

[2] ACI 440.2R-08. Guide for the design and construction of externally bonded FRP system for strengthening concrete structures, ACI committee 440. Farmington Hills (MI): American Concrete Institute; p. 76. (2008).
[3] CHOU, J., et al.: Fatigue behavior of reinforced concrete beams strengthened with prestressed near-surface-mounted carbon-fiber-reinforced polymer strips. Composite Structures 308 (2023): 116689.
[4] AL-BAYATI, A. F.: Shear strength of reinforced concrete beam–column joints. Asian Journal of Civil Engineering 24.1 (2023): 319-351.
[5] RAO, B. T. M. - RAHUL, R. M. - PRAKASH, S. S.: Experimental Investigation on Flexural Behaviour of RC Beams Strengthened with Various FRP Composite Configurations. Fiber Reinforced Polymeric Materials and Sustainable Structures. Singapore: Springer Nature Singapore, 2023. 121-128.
[6] ABDALLAH, M. et al.: Effect of the strengthening patterns on the flexural performance of RC continuous beams using FRP reinforcements. Engineering Structures 280 (2023): 115657.
[7] KELLER, T. - SCHAUMANN, E. - VALLÉE, T.: Flexural behavior of a hybrid FRP and lightweight concrete sandwich bridge deck. Composites Part A: Applied Science and Manufacturing 38.3 (2007): 879-889.
[8] FARIA, D. MV. - LÚCIO, V. JG. - RAMOS, P. A.: Strengthening of flat slabs with post-tensioning using anchorages by bonding. Engineering Structures 33.6 (2011): 2025-2043.
[9] AL-ROUSAN, R. - ISSA, M. - SHABILA, H.: Performance of reinforced concrete slabs strengthened with different types and configurations of CFRP. Composites Part B: Engineering 43.2 (2012): 510-521.
[10] HEMANTH, J.: Compressive strength and microstructural properties of lightweight high-strength cement mortar reinforced with eloxal. Materials & design 27.8 (2006): 657-664.
[11] DAUD, S. A. - RAID, A. D. - AL-AZZAWI, A. A.: Behavior of reinforced concrete solid and hollow beams that have additional reinforcement in the constant moment zone. Ain Shams Engineering Journal 12.1 (2021): 31-36.
[12] AL-AZZAWI, A. A. - RAID, A. D. - SULTAN, A. D.: Behavior of tension lap spliced sustainable concrete flexural members. Advances in concrete construction 9.1 (2020): 83-92.
[13] CANTONE, R. et al.: Enhancing punching strength and deformation capacity of flat slabs. ACI structural journal 116.ARTICLE (2019): 261-274.
[14] AL-AZZAWI, A. A.: Free vibration of simply supported beam on elastic foundations. Al-Nahrain Journal for Engineering Sciences 20.2 (2017): 353-357.
[15] NAJM, I. N. - RAID, A. D. - AL-AZZAWI, A. A.: Behavior of reinforced concrete segmental hollow core slabs under monotonic and repeated loadings. Structural Monitoring and Maintenance 6.4 (2019): 269.
[16] AL-BAYATI, A. F. - TAKI, Z. N. M.: Shear strength prediction of steel fiber reinforced concrete beams without transverse reinforcements. Asian Journal of Civil Engineering 25.2 (2024): 1857-1875.
[17] DAUD, R. A. - CUNNINGHAM, L. S. - WANG, Y. C.: New model for post-fatigue behaviour of CFRP to concrete bond interface in single shear. Composite Structures 163 (2017): 63-76.
[18] DAUD, R. A. - SULTAN, A. D. - AL-AZZAWI, A. A.: Tension stiffening evaluation of steel fibre concrete beams with smooth and deformed reinforcement. Journal of King Saud University-Engineering Sciences 33.3 (2021): 147-152.
[19] ABOUL-NOUR, L. - EISA, A. - EL-GHAMRY, A.: Structural behavior of Lightweight and High strength Layered Hollow Core Slabs. Frattura ed Integrità Strutturale 63 (2023): 134-152.
[20] KHAMIS, M. K. et al.: Experimental behavior based on effective slab width acting as a flange with supporting steel beams in composite floors with openings. Frattura ed Integrità Strutturale 16.61 (2022): 308-326.
[21] DA COSTA, P. O. B. - RÚBIA, M. B. - DE MIRANDA SALEME GIDRÃO, G.: Behavior assessment of asymmetrical building with concrete damage plasticity (CDP) under seismic load. Frattura ed Integrità Strutturale 16.61 (2022): 108-118.
[22] THANOON, W. A. et al.: Repair and structural performance of initially cracked reinforced concrete slabs. Construction and Building Materials 19.8 (2005): 595-603.
[23] FORET, G. - LIMAM, O.: Experimental and numerical analysis of RC two-way slabs strengthened with NSM CFRP rods. Construction and Building Materials 22.10 (2008): 2025-2030.
[24] EL MAADDAWY, T. - SOUDKI, K.: Strengthening of reinforced concrete slabs with mechanically-anchored unbonded FRP system. Construction and Building Materials 22.4 (2008): 444-455.
[25] KOWALSKY, M. J. - PRIESTLY, MJ. N. - SEIBLE, F.: Shear and flexural behavior of lightweight concrete bridge columns in seismic regions. ACI Structural Journal 96 (1999): 136-148.

[26] ZHANG, J. et al.: Introducing ductile strip for durability enhancement of concrete slabs. Journal of Materials in Civil Engineering 14.3 (2002): 253-261.
[27] BELARBI, A. - ACUN. B.: FRP systems in shear strengthening of reinforced concrete structures. Procedia Engineering 57 (2013): 2-8.
[28] ASKAR, M. K. - HASSAN, A. F. - AL-KAMAKI, Y. SS: Flexural and shear strengthening of reinforced concrete beams using FRP composites: A state of the art. Case Studies in Construction Materials 17 (2022): e01189.
[29] MADQOUR, M. – FAWZI, K. – HASSAN, H.: Finite element modeling of flexural behavior of reinforced concrete beams externally strengthened with CFRP sheets. Frattura ed Integrità Strutturale 16.59 (2022): 62-77.
[30] MARFIA, S. - SACCO, E. - TOTI, J.: An approach for the modeling of interface-body coupled nonlocal damage. Frattura ed Integrità Strutturale 4.12 (2010): 13-20.
[31] ACI Committee 318. "Building Code Requirements for Structural Concrete (ACI 318-19): An ACI Standard; Commentary on Building Code Requirements for Structural Concrete (ACI 318R-19)." American Concrete Institute, 2019.
[32] THOMSEN, H. et al.: Failure mode analyses of reinforced concrete beams strengthened in flexure with externally bonded fiber-reinforced polymers. Journal of composites for construction 8.2 (2004): 123-131.
[33] SPADEA, G. - SWAMY, R. N. - BENCARDINO, F.: Strength and ductility of RC beams repaired with bonded CFRP laminates. Journal of Bridge Engineering 6.5 (2001): 349-355.
[34] LING, J. H. - LIM, Y. T. - JUSLI. E.: Methods to determine ductility of structural members: a review. Journal of the Civil Engineering Forum. Vol. 9. No. 2. Universitas Gadjah Mada, 2023.
[35] ZOU, P. XW.: Flexural behavior and deformability of fiber reinforced polymer prestressed concrete beams. Journal of composites for Construction 7.4 (2003): 275-284.
[36] TANN, D. B. - DAVIES, P. - Delpak, R.: A review of ductility determination of FRP strengthened flexural RC elements. Fibre-Reinforced Polymer Reinforcement for Concrete Structures: (In 2 Volumes) (2003): 347-356.
[37] HASSAN, N. Z. - HALA, M. I. - AMANY, M. S.: Study behavior of hollow reinforced concrete beams. Int. J. Curr. Eng. Technol 8.6 (2018): 1640-1651.